Optical-absorption spectra in fullerenes C_{60} and C_{70}: Effects of Coulomb interactions, lattice fluctuations, and anisotropy

Kikuo Harigaya* and Shuji Abe
Fundamental Physics Section, Physical Science Division, Electrotechnical Laboratory, Umezono 1-1-4, Tsukuba, Ibaraki 305, Japan
(Received 31 January 1994)

Effects of Coulomb interactions and lattice fluctuations in the optical-absorption spectra of C_{60} and C_{70} are theoretically investigated by using a tight-binding model with long-range Coulomb interaction and bond disorder. Anisotropy effects in C_{70} are also considered. Optical spectra are calculated by using the Hartree-Fock approximation followed by the configuration interaction method. The main conclusions are as follows. (1) The broad peaks at excitation energies, 3.7, 4.7, and 5.7 eV, observed in experiments of C_{60} molecules in a solution, are reasonably described by the present theory. Peak positions and relative oscillator strengths are in overall agreement with the experiments. The broadening of peaks by lattice fluctuations is well simulated by the bond disorder model. (2) The optical gap of C_{70} is larger when the electric field of light is parallel to the long axis of the molecule. The shape of the frequency dispersion also depends on the orientation of the molecule. These properties are common in the free-electron model and the model with Coulomb interactions. (3) The spectrum of C_{70} averaged over bond disorder and random orientations is compared with experiments in a solution. There is an overall agreement about the spectral shape. Differences in the spectra of C_{60} and C_{70} are discussed in connection with the associated symmetry reduction.

I. INTRODUCTION

Recently, fullerenes C_N ($N = 60, 70, 76$, and so on) with hollow cage structures have been intensively investigated. Many optical experiments have been performed, and interesting properties originating from π electrons delocalized on molecule surfaces have been revealed. They include the optical-absorption spectra of C_{60} (Refs. 1 and 2) and C_{70},[1] and the large optical nonlinearity of C_{60}.[3,4] The nonlinearity in the third harmonic generation (THG) is of the order 10^{-11} esu, and this largeness is attractive in scientific as well as technological interests. The C_{70} thin films show a large THG magnitude extending to 10^{-11} esu also.[5] Therefore, the fullerene family is generally attractive for possible application to nonlinear optical devices in the near future.

In order to analyze the optical properties and to clarify mechanisms of the large nonlinearity, we have studied the linear absorption and the THG of C_{60} by using a tight-binding model[6] and a model with a long-range Coulomb interaction.[7] A free-electron model yields the THG magnitudes which are in agreement with the experiment of C_{60},[2] while the calculated linear absorption spectrum is not in satisfactory agreement with experiments.[6] If Coulomb interactions are taken into account, the absorption spectra are in overall agreement with the experiment, although the magnitude of the THG decreases by a factor of about 0.1.[7]

The first purpose of this paper is to report the details of the analysis of optical-absorption spectra of C_{60}. In the previous paper,[7] the effects of the long-ranged Coulomb interactions have been considered in the tight-binding model for a single molecule. The model has been analyzed by the restricted Hartree-Fock approximation followed by the single excitation configuration interaction method (single CI).[8] We use the same method in this paper. In the experiments of actual materials, the optical spectra become broad mainly due to the lattice fluctuations. We are going to simulate the effects by using the bond disorder model with a Gaussian distribution. We will take a sample average over disorder potentials. This method has been used in order to describe the optical properties of conjugated polymers.[9,10] We will show that the main features observed in the experiments of C_{60} molecules in a solution[2] are reasonably described by the present theory. Speaking in detail, peak positions in the frequency dispersion of the spectra agree well with the experiment. The relative oscillator strengths are in overall agreement with the experimental data. Furthermore, the broadening of absorption peaks by lattice fluctuations is well simulated by the bond disorder model with a reasonable disorder strength.

Second, we extend the calculations to one of the higher fullerenes, C_{70}. The molecular shape becomes elongated in going from C_{60} to C_{70}. Then, we expect that the optical response varies depending on the molecular orientation relative to the electric field of light. We will discuss the anisotropy for the free-electron model and for the model with the Coulomb potentials. It is found that the optical gap is larger when the electric field is parallel to the long axis of the C_{70} molecule. The line shape of the absorption spectrum is anisotropic, too. These properties do not depend on whether the Coulomb interactions are present or not. We expect that the anisotropy will be observed in the solids of C_{70}.

Finally, we consider a situation in which the C_{70} molecule is rotated randomly and the anisotropy of the optical absorption is averaged out. The optical spectrum

calculated by the model with Coulomb interactions and disorder potentials are compared with the experimental data[1] for molecules in a solution. We will conclude that there is an overall agreement. The absorption around 2.7 eV in the experiment can be interpreted as an allowed transition. There are several allowed transitions below the energy 2.7 eV, but their oscillator strengths are smaller. We can relate the spectra of C_{60} and C_{70} by considering the associated symmetry reduction.

We shall report calculations in the following way. In the next section, our model and its meaning are explained. The calculation method of the single CI is also summarized. In Sec. III, we report about C_{60} and compare with the experiment. In Sec. IV, we describe the optical spectra of C_{70}. The paper is closed with several remarks in the final section.

II. MODEL AND FORMALISM

In order to consider optical spectra of C_{60} and C_{70}, we use the following Hamiltonian:

$$H = H_0 + H_{\rm bond} + H_{\rm int}. \tag{1}$$

The first term H_0 of Eq. (1) is the tight-binding model. We use the following form for C_{60}:

$$H_0 = \sum_{\langle i,j\rangle,\sigma}{}^{D}(-t_D)(c^\dagger_{i,\sigma}c_{j,\sigma} + \text{H.c.}) + \sum_{\langle i,j\rangle,\sigma}{}^{S}(-t_S)(c^\dagger_{i,\sigma}c_{j,\sigma} + \text{H.c.}), \tag{2}$$

where $c_{i,\sigma}$ is an annihilation operator of a π electron at site i with spin σ; the sum with the symbol D (or S) is taken over all the pairs $\langle i,j\rangle$ of neighboring atoms with a double (or single) bond; and $t_D = t + (2/3)t'$ and $t_S = t-(1/3)t'$ are the hopping integrals. The mean hopping is taken as t. In this paper, we use the difference between t_D and t_S, $t' = 0.1t$ as a typical value. The choice of t' does not affect the results as strongly, because main contributions come from the strong Coulomb potential. We use the next form for C_{70},

$$H_0 = -t\sum_{\langle i,j\rangle,\sigma}(c^\dagger_{i,\sigma}c_{j,\sigma} + \text{H.c.}), \tag{3}$$

assuming a constant hopping integral. We could use a realistic combination of hoppings, but the results do not change as much such as in the C_{60} case. Effects of zero point vibrations and thermal fluctuation of the lattice are modeled by the bond disorder model which is the second term of Eq. (1),

$$H_{\rm bond} = \sum_{\langle i,j\rangle,\sigma}\delta t_{i,j}(c^\dagger_{i,\sigma}c_{j,\sigma} + \text{H.c.}). \tag{4}$$

Here, $\delta t_{i,j}$ is the disorder potential at the bond $\langle i,j\rangle$. We can estimate the strength of the disorder (standard deviation) t_s from the results[11] by the extended Su-Schrieffer-Heeger (SSH) model.[12] The value would be $t_s \sim 0.05 - 0.1t$. This is of the similar magnitude as in the fullerene tubules and conjugated polymers.[13] We shall treat interactions among π electrons by the following model:

$$H_{\rm int} = U\sum_i(c^\dagger_{i,\uparrow}c_{i,\uparrow} - \tfrac{1}{2})(c^\dagger_{i,\downarrow}c_{i,\downarrow} - \tfrac{1}{2}) + \sum_{(i,j),i\neq j}W(r_{i,j})\left(\sum_\sigma c^\dagger_{i,\sigma}c_{i,\sigma} - 1\right)\left(\sum_\tau c^\dagger_{j,\tau}c_{j,\tau} - 1\right), \tag{5}$$

where $r_{i,j}$ is the distance between the ith and jth sites and

$$W(r) = \frac{1}{\sqrt{(1/U)^2 + (r/r_0V)^2}} \tag{6}$$

is the Ohno potential. The quantity U is the strength of the onsite interaction, V means the strength of the long-range Coulomb interaction, and r_0 is the average bond length.

The model is treated by the Hartree-Fock approximation and the single CI.[8] After the Hartree-Fock approximation $H \Rightarrow H_{\rm HF}$, we divide the total Hamiltonian as $H = H_{\rm HF} + H'$. The term H' becomes

$$H' = U\sum_i(c^\dagger_{i,\uparrow}c_{i,\uparrow} - \rho_{i,\uparrow})(c^\dagger_{i,\downarrow}c_{i,\downarrow} - \rho_{i,\downarrow}) + \sum_{(i,j),i\neq j}W(r_{i,j})\Big[\sum_{\sigma,\tau}(c^\dagger_{i,\sigma}c_{i,\sigma} - \rho_{i,\sigma})(c^\dagger_{j,\tau}c_{j,\tau} - \rho_{j,\tau}) + \sum_\sigma(\tau_{i,j,\sigma}c^\dagger_{j,\sigma}c_{i,\sigma} + \tau_{j,i,\sigma}c^\dagger_{i,\sigma}c_{j,\sigma} - \tau_{i,j,\sigma}\tau_{j,i,\sigma})\Big], \tag{7}$$

where $\rho_{i,\sigma} = \langle c^\dagger_{i,\sigma}c_{i,\sigma}\rangle$ and $\tau_{i,j,\sigma} = \langle c^\dagger_{i,\sigma}c_{j,\sigma}\rangle$. When we write the Hartree-Fock ground state $|g\rangle = \prod_{\lambda:\text{occupied}}c^\dagger_{\lambda,\uparrow}c^\dagger_{\lambda,\downarrow}|0\rangle$ and the single electron-hole excitations $|\mu\lambda\rangle = c^\dagger_{\mu,\sigma}c_{\lambda,\tau}|g\rangle$ (μ means an unoccupied state; we assume both singlet and triplet excitations in this abbreviated notation), the matrix elements of the Hartree-Fock part and the excitation Hamiltonian become as follows:

$$\langle\mu'\lambda'|(H_{\rm HF} - \langle H_{\rm HF}\rangle)|\mu\lambda\rangle = \delta_{\mu',\mu}\delta_{\lambda',\lambda}(E_\mu - E_\lambda), \tag{8}$$

$$\langle\mu'\lambda'|(H'-\langle H'\rangle)|\mu\lambda\rangle\rangle = 2J\delta_S - K, \tag{9}$$

where E_μ is the energy of the Hartree-Fock state, $\delta_S = 1$ for spin singlet, $\delta_S = 0$ for spin triplet, and

$$J(\mu',\lambda';\mu,\lambda) = \sum_{i,j} V_{i,j}\langle\mu'|i\rangle\langle\lambda'|i\rangle\langle j|\mu\rangle\langle j|\lambda\rangle \ , \tag{10}$$

$$K(\mu',\lambda';\mu,\lambda) = \sum_{i,j} V_{i,j}\langle\mu'|j\rangle\langle\lambda'|i\rangle\langle j|\mu\rangle\langle i|\lambda\rangle \ , \tag{11}$$

with $V_{i,i} = U$, $V_{i,j} = W(r_{i,j})$ for $i \neq j$. The diagonalization of the total Hamiltonian H gives the set of the excited states $\{|\kappa\rangle\}$ within the single CI method. In the actual calculation, we limit the spin configurations to the singlet excitations.

The absorption spectrum in the case of the electric field parallel to the x axis is proportional to

$$\sum_\kappa E_\kappa P(\omega - E_\kappa)\langle g|x|\kappa\rangle\langle\kappa|x|g\rangle. \tag{12}$$

Here, $P(\omega) = \gamma/[\pi(\omega^2+\gamma^2)]$ is the Lorentzian distribution (γ is the width), E_κ is the electron-hole excitation energy, and $|g\rangle$ means the ground state.

In this paper, all the quantities with the energy dimension are shown in the units of t. We varied the parameters of the Coulomb interaction within $0 \leq V \leq U \leq 5t$, and we report here the two representative cases: $U = V = 0$ and $U = 2V = 4t$. Results in the latter case turn out to be in overall agreement with experiments.

III. OPTICAL ABSORPTION IN C_{60}

This section is devoted to the optical spectra of C_{60}, the structure of which is shown in Fig. 1(a). The calculated spectra are nearly isotropic independent of the direction of the electric field against the molecular orientation.

A. Coulomb interaction effects

The dispersion of the optical absorption is calculated for the free-electron case $U = V = 0$, and displayed in Fig. 2(a). The Lorentzian broadening $\gamma = 0.01t$ is used. The distribution of the relative oscillator strength and the positions of the peaks agree with those in the previous calculations.[6] The second peak at about $1.2t$ has the largest oscillator strength.

Figure 2(b) shows the absorption for $U = 4t$ and $V = 2t$. There are several peaks, among which the peak at $\sim 2.6t$ has the largest oscillator strength. This is in contrast to the free-electron case ($U = V = 0$), where the oscillator strength is the largest at around $1.2t$. The Coulomb interaction tends to reduce the oscillator strengths of the lower-energy peaks and to enhance those of the higher-energy peaks. In addition, it shifts overall peak positions to higher energies. Qualitatively similar results have been reported in terms of the random phase approximation.[14] The overall distribution of the oscillator strengths in Fig. 2(b) is in good agreement with experiments[2] when we assume $t = 1.8$ eV. The origin of the large broadening of the peaks may be lattice fluctuations. This is to be discussed in the next subsection.

Now, we can estimate a dielectric constant ϵ. The magnitude of the Coulomb interaction at the mean carbon bond length is $W(r_0) = UV/\sqrt{U^2+V^2}$. This gives an estimate: $\epsilon = e^2/[r_0 W(r_0)] = 3.11$. The long distance limit $W(r \gg r_0) \sim Vr_0/r$ gives $\epsilon = 2.80$. The independent study of the lifetime of positrons in C_{60} gives the high frequency dielectric constant $\epsilon_\infty \sim 3.5$.[15] Therefore, the present estimation of the dielectric constant near the value 3 would be reasonable.

B. Lattice fluctuation effects

Here, we should like to take into account the lattice fluctuation effects. We simulate the effects by the bond disorder model with a Gaussian distribution. The application of the model has been successful in describing the lattice fluctuation effects in conjugated polymers.[9] The estimation by the results of the extended SSH model for C_{60} gives the order $t_s \sim 0.05 - 0.1t$.[11] We change the disorder strength around these values. Averaging over 100 samples turned out to be enough to obtain the smooth optical spectra.

Figure 2(c) shows the calculated optical spectrum for

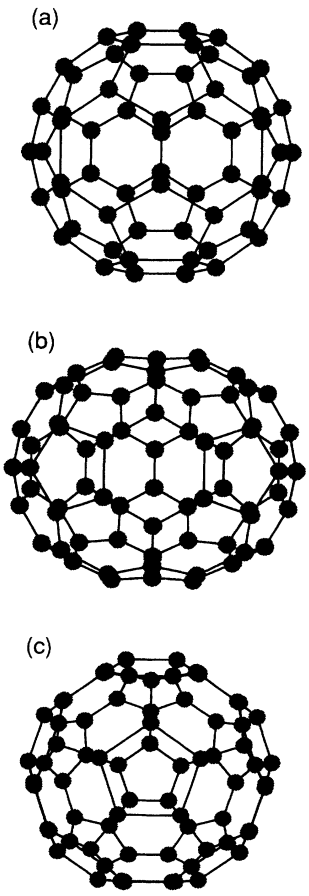

FIG. 1. Molecular structures for (a) C_{60}, and (b) and (c) C_{70}. In (b), the long axis (x axis) penetrates from the left to the right of the figure. The mirror symmetry planes are perpendicular to the figure. In (c), the C_{70} is projected along the long axis.

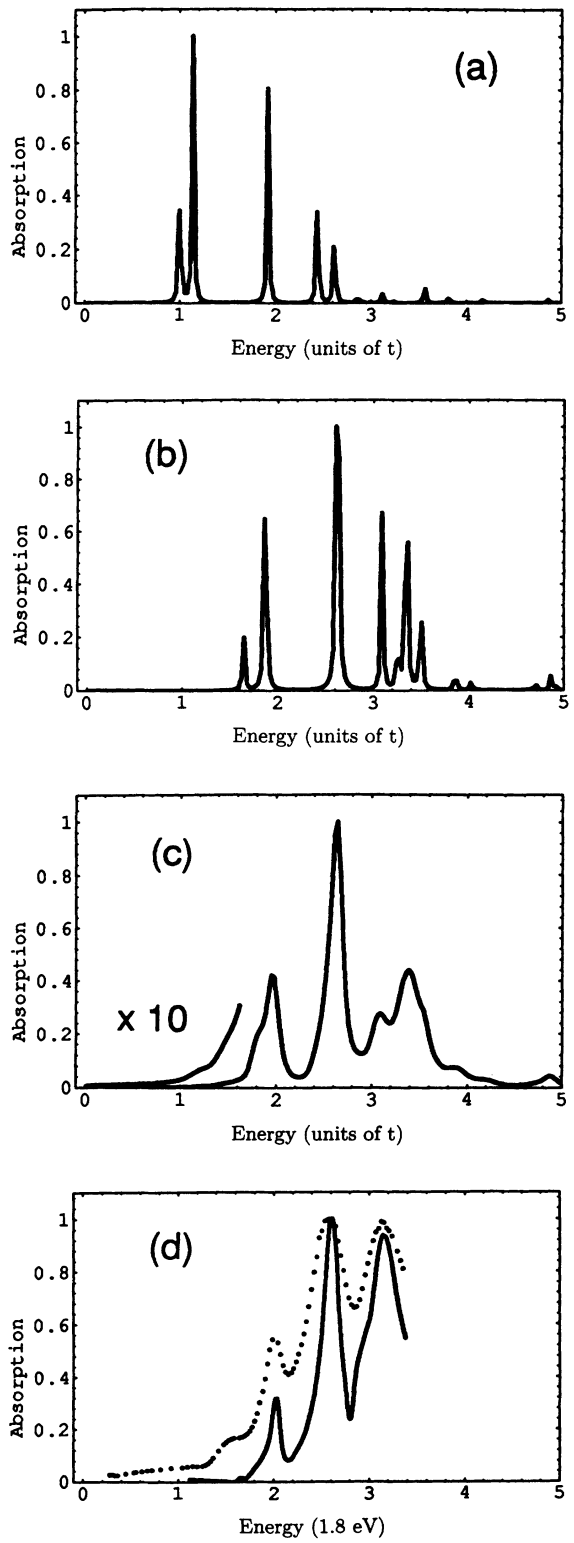

FIG. 2. Optical-absorption spectra for C_{60} shown in arbitrary units. The abscissa is scaled by t. The spectra are calculated with the parameters (a) $U = V = 0$, (b) and (c) $U = 4t$ and $V = 2t$. The Lorentzian broadening $\gamma = 0.01t$ is used. In (c), lattice fluctuations are taken into account by the bond disorder of the strength $t_s = 0.09t$. (d) The experimental spectra (Ref. 2) of molecules in a solution (solid line) and of a C_{60} film (dotted line). We use $t = 1.8$ eV.

$t_s = 0.09t$. For comparison, we show in Fig. 2(d) the experimental data obtained by Ren *et al.* for C_{60} in a solution and a C_{60} thin film.[2] The data are shown for comparison assuming $t = 1.8$ eV. Due to the broadening, the peaks near the energy $1.8t$ in Fig. 2(b) merge into a single broad feature in Fig. 2(c). The several peaks around $3.4t$ obtain the same effect as well. Overall, there are three main features in the energy dependence of the calculated data. Their positions in the energy agree well with the experimental data, $2.0t$, $2.6t$, and $3.1t$, obtained from the solution. The relative oscillator strengths fairly agree also. Furthermore, the widths of the features can be well simulated by the broadening from the bond disorder model. Experimentally, the peaks would be broadened by various kinds of phonon modes: intermolecular libration and intramolecular vibrations. They give rise to many sidebands, which broaden into several main features. The disorder strength, adopted here, simulates well the total broadening as the net contribution from the various phonon modes.

In the solid, the broadening is larger and a broad hump appears around the energy 2.8 eV ($= 1.5t$), as is shown in Fig. 2(d). There is a tiny structure at 3 eV in the corresponding region of the absorption spectrum of C_{60} in a solution [Fig. 2(d) and Ref. 17]. We assume that the forbidden transitions in that energy region become partially allowed due to lattice fluctuations or intermolecular interactions. If the lattice fluctuations are effective, the effect can be simulated by the bond disorder model. In Fig. 2(c), the absorption in the low-energy part multiplied by the factor 10 is also shown. The several forbidden transitions around $1.2t - 1.6t$ become allowed by the disorder, giving rise to an absorption tail in the lower-energy region. The relative magnitude is similar to the solution data shown in Fig. 2(d). This might be also the origin of the 2.8 eV hump in the solid. However, the strength of the absorption relative to the main peaks in our theory is about one order of magnitude smaller than that in the experiment. If we increase disorder drastically to explain the magnitude, we get absorption peaks that are too broad compared with the experiments. This is true for all the cases of Coulomb interaction parameters we tried. Therefore, it seems difficult to explain the oscillator strength of the partially allowed transitions in solids quantitatively. Additional effects such as intermolecular interactions will be necessary, and this problem will be investigated in a separate paper.[16] We note that the C_{60} oxide shows a weak absorption peak in a similar energy region.[18] This could also be interpreted by using a model with impurities.

IV. OPTICAL ABSORPTION IN C_{70}

A. Anisotropy effects

The C_{70} molecule has an ellipsoidal shape. Figures 1(b) and (c) display the molecule. We locate the long axis of the molecule along the x direction. Figure 1(b) shows the molecule that is projected along the z axis. The x axis goes from the left to the right of the

figure. Figure 1(c) is the molecule projected along the x axis. We expect that the absorption becomes anisotropic with respect to the direction of the electric field of light. We look at anisotropy effects in the free-electron model as well as in the model with Coulomb interactions.

Figures 3(a), (b), and (c) show absorption spectra of the free-electron case when the electric field is in the x, y, and z directions, respectively. Figures 3(b) and (c) have almost the same spectral shape. But, the spectral shape is very different when the electric field is parallel to the long axis. The optical gap is about $0.7t$ in Fig. 3(a), while it is about $0.6t$ in Figs. 3(b) and (c). This accords with the result of the recent Hückel calculation[19] in that the optical gap of C_{70} is larger when the electric field is parallel to the long axis of the molecule.

Next, we shall turn to Coulomb interaction effects. We display the optical spectra for $U = 4t$ and $V = 2t$. We will later find that these parameters are appropriate for C_{70} also. Figures 4(a), (b), and (c) show the spectra for the respective molecular orientations corresponding to Figs. 3(a)–(c). It seems that there is a strong anisotropy when the Coulomb interactions are present, too. The op-

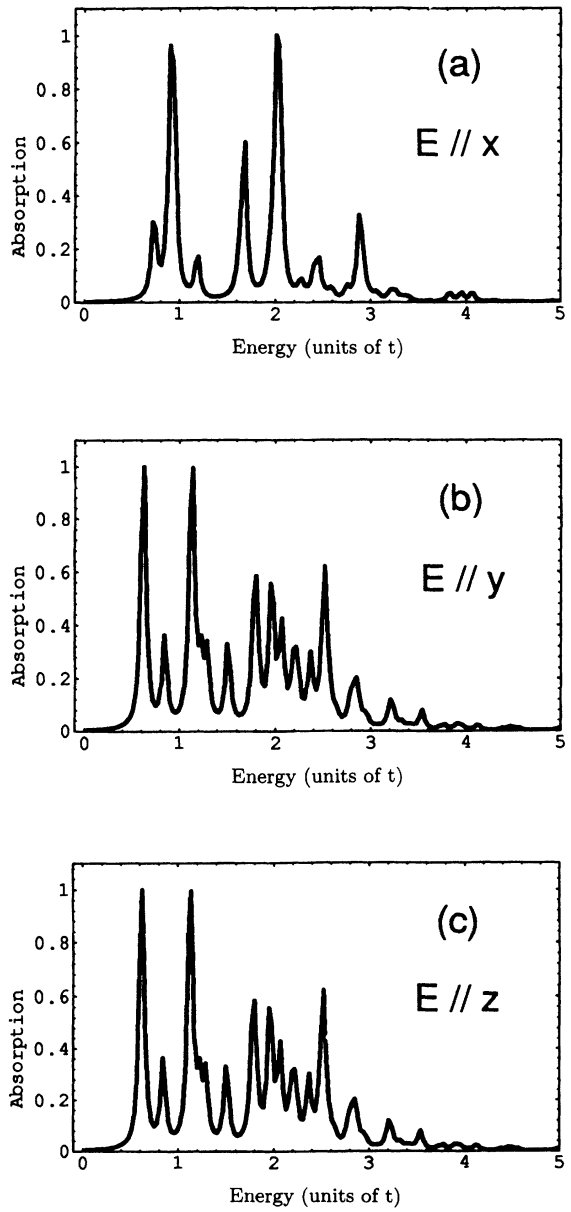

FIG. 3. Optical-absorption spectra for C_{70} shown in arbitrary units. The abscissa is scaled by t. The interaction strengths are $U = V = 0$. The Lorentzian broadening $\gamma = 0.01t$ is used. In (a), (b), and (c), the electric field is parallel to the x, y, and z axes, respectively.

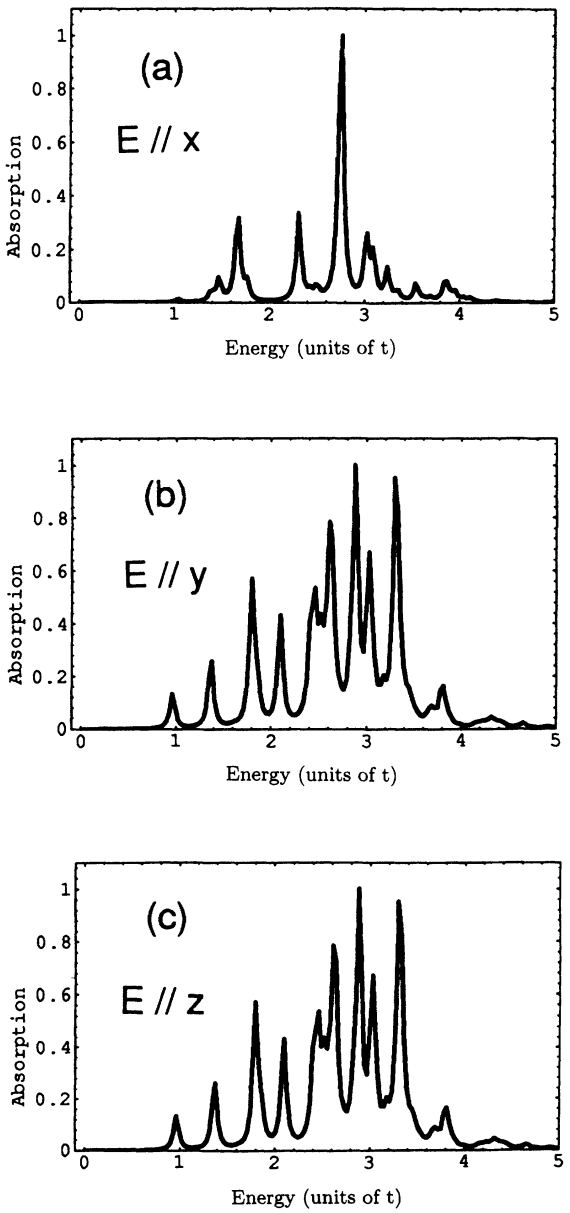

FIG. 4. Optical-absorption spectra for C_{70} shown in arbitrary units. The abscissa is scaled by t. The interaction strengths are $U = 4t$ and $V = 2t$. The Lorentzian broadening $\gamma = 0.01t$ is used. In (a), (b), and (c) the electric field is parallel to the x, y, and z axes, respectively.

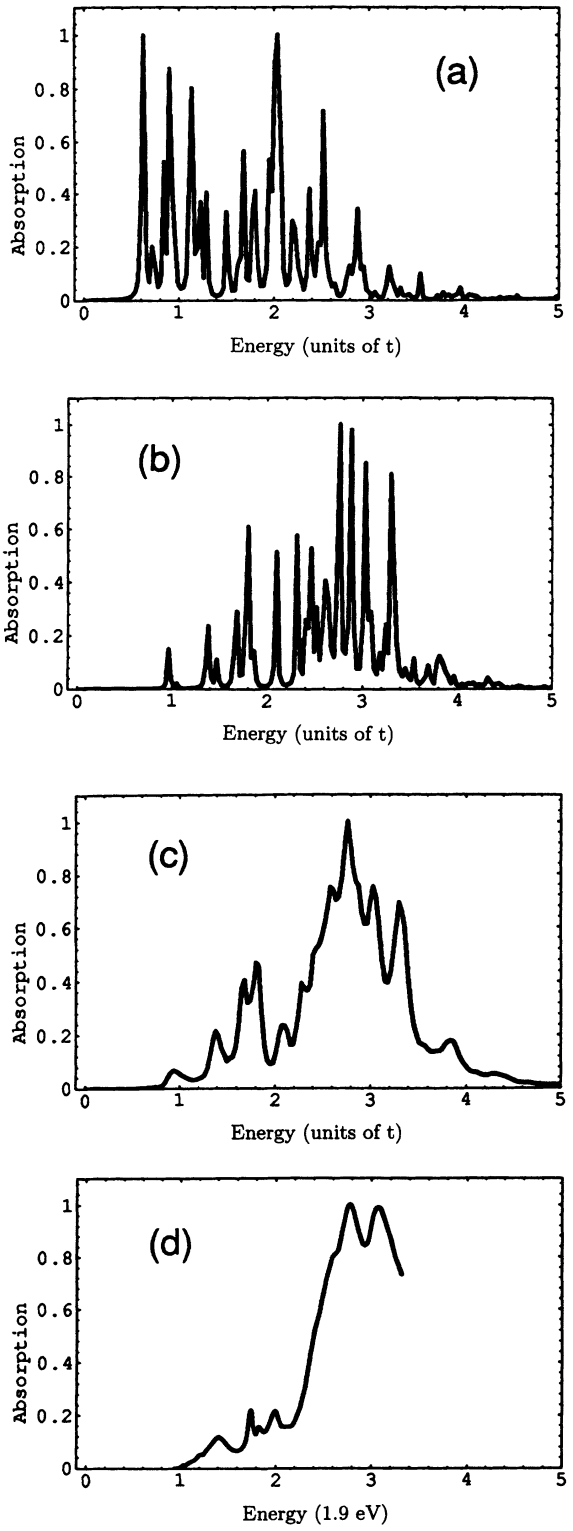

FIG. 5. Orientationally averaged optical-absorption spectra for C_{70} shown in arbitrary units. The abscissa is scaled by t. The spectra are calculated with the parameters (a) $U = V = 0$, (b) and (c) $U = 4t$ and $V = 2t$. The molecule is rotated randomly in order to average the anisotropy. The Lorentzian broadening $\gamma = 0.01t$ is used. In (c), lattice fluctuations are taken into account by the bond disorder of the strength $t_s = 0.09t$. (d) The experimental spectrum (Ref. 1) of molecules in a solution. We use $t = 1.9$ eV.

tical gap in Fig. 4(a) is about $1.1t$ with a weak absorption peak. It is about $1.0t$ in Figs. 4(b) and (c). Therefore, the optical gap becomes larger when the electric field is parallel to the long axis of the molecule. This property does not change whether there are Coulomb interactions or not. We highly expect that the anisotropy will be clearly observed in the solid of C_{70}.

B. Orientationally averaged spectra

1. *Coulomb interaction effects*

The optical-absorption data have been reported for molecules in solution.[1] In order to compare the present theory with the experiment, we have rotated the molecule randomly and averaged the spectra over 100 orientations. Averaged data without bond disorder are shown in Figs. 5(a) and (b). We use the Lorentzian broadening $\gamma = 0.01t$ as before. Figure 5(a) is for the free-electron case, and Fig. 5(b) is for the Coulomb interaction strengths $U = 4t$ and $V = 2t$. We can easily see that the peaks in the three figures of Fig. 3 remain in Fig. 5(a). The same thing can be said about the relation between Fig. 4 and Fig. 5(b). The effects of the Coulomb interactions are similar to those of the C_{60} case: the Coulomb potentials tend to shift peaks to higher energies, and oscillator strengths at higher energies have relatively larger weight than in the free-electron case. The shift is due to the fact that the intersite Coulomb interactions give rise to bond order parameters in the Hartree-Fock approximation. The bond order effectively enhances the intersite hopping integrals, and thus the energy gap.

2. *Lattice fluctuation effects*

Now, we treat lattice fluctuation effects by using the bond disorder model. As we expect that the width of lattice fluctuations in C_{70} is similar to that in C_{60} even if the molecular structure is different, we assume the same $t_s = 0.09t$ in this calculation again. The orientation of the molecule and disorder potentials are changed 100 times, and the optical spectra are averaged.

Figure 5(c) shows the calculated optical absorption. Figure 5(d) shows the experimental data of C_{70} in a solution taken from Ref. 1. The abscissa is scaled by using $t = 1.9$ eV. The optical gap near $1.0t$ accords well with the experiment. The small peaks around $1.8t$ may correspond to those of the experiment in the similar energy region. Commonly, there is a dip of the optical absorption at about $2.0t$ in the calculation and experiment. There is a maximum at $2.8t$ in the two data. Therefore, we conclude that there is an overall agreement between the calculation and the experiment. The quantum lattice fluctuation effects are also simulated well by the bond disorder model.

V. CONCLUDING REMARKS

The most striking difference between optical spectra of C_{60} solution and of C_{60} solids is that the feature around

2.8 eV has the strong oscillator strength only in solids. In the present calculation for $U = 4t$ and $V = 2t$ without disorder, there are dipole forbidden transitions at the corresponding energy. The disorder makes these transitions partially allowed. We have discussed that this effect is one of the origins which make the forbidden transitions observed. However, the theoretical oscillator strengths seem to be smaller by an order of magnitude than that in the experiments. We need further study in order to solve this problem. For example, we are now studying intermolecular interaction effects in addition to lattice fluctuations. This will be reported separately.[16]

We have discussed that the absorption near 2.8–3.0 eV of C_{60} might originate from partially allowed transitions by lattice fluctuations and/or intermolecular hopping interactions. However, origins are somewhat controversial. For example, the experimental[20] and theoretical[21] papers have assigned the absorption as the allowed transitions which includes interactions with intramolecular phonons. Further studies are necessary to resolve the problem.

The absorption spectra of C_{70} become highly anisotropic depending on the orientation of the molecule relative to the polarization of light. Now, single crystals of C_{70} have been made and their optical data have been reported.[5] Therefore, an extension of the present calculations to C_{70} solids is quite interesting. We expect that the anisotropy of the optical spectra of the molecule will remain in solids, too.

In view of the agreement of our theory with experiments in C_{60} and C_{70}, it is very interesting to look at optical properties and excitonic effects of higher fullerenes where the number of carbons is larger than 70. The method of the single CI should be valid enough in these systems, too. The number of isomers rapidly increases as the carbon number increases as 76, 78, 82, 84, and so on. The calculated optical data will reflect the electronic and lattice structures of isomers, and they will be mutually different. Thus, the calculations will be useful in order to distinguish isomers by using optical experiments.

ACKNOWLEDGMENTS

The authors acknowledge helpful correspondence with Dr. Mitsutaka Fujita. They also thank Mr. Mitsuho Yoshida for providing them with the molecular coordinate of C_{70} which is generated by the program[22] based on the projection method on the triangular[22] and honeycomb lattices.[23] Part of this work was done while one of the authors (K.H.) was staying at the University of Sheffield, United Kingdom. He acknowledges the hospitality that he obtained from the University.

*Electronic address: harigaya@etl.go.jp.

[1] J. P. Hare, H. W. Kroto, and R. Taylor, Chem. Phys. Lett. **177**, 394 (1991).
[2] S. L. Ren, Y. Wang, A. M. Rao, E. McRae, J. M. Holden, T. Hager, KaiAn Wang, W. T. Lee, H. F. Ni, J. Selegue, and P. C. Eklund, Appl. Phys. Lett. **59**, 2678 (1991).
[3] J. S. Meth, H. Vanherzeele, and Y. Wang, Chem. Phys. Lett. **197**, 26 (1992).
[4] Z. H. Kafafi, J. R. Lindle, R. G. S. Pong, F. J. Bartoli, L. J. Lingg, and J. Milliken, Chem. Phys. Lett. **188**, 492 (1992).
[5] F. Kajzar, C. Taliani, R. Danieli, S. Rossini, and R. Zamboni (unpublished).
[6] K. Harigaya and S. Abe, Jpn. J. Appl. Phys. **31**, L887 (1992).
[7] K. Harigaya and S. Abe, J. Lumin. (to be published).
[8] S. Abe, J. Yu, and W. P. Su, Phys. Rev. B **45**, 8264 (1992).
[9] S. Abe, M. Schreiber, W. P. Su, and J. Lu, Mol. Cryst. Liq. Cryst. **217**, 1 (1992).
[10] K. Harigaya, A. Terai, Y. Wada, and K. Fesser, Phys. Rev. B **43**, 4141 (1991).
[11] B. Friedman and K. Harigaya, Phys. Rev. B **47**, 3975 (1993); K. Harigaya, *ibid.* **48**, 2765 (1993).
[12] W. P. Su, J. R. Schrieffer, and A. J. Heeger, Phys. Rev. B **22**, 2099 (1980).
[13] R. H. McKenzie and J. W. Wilkins, Phys. Rev. Lett. **69**, 1085 (1992).
[14] G. F. Bertsch, A. Bulgac, D. Tománek, and Y. Wang, Phys. Rev. Lett. **67**, 2690 (1991); Y. Wang, G. F. Bertsch, and D. Tománek, Z. Phys. D **25**, 181 (1993).
[15] S. Ishibashi, N. Terada, M. Tokumoto, N. Kinoshita, and H. Ihara, J. Phys. Condens. Matter **4**, L169 (1992).
[16] S. Abe and K. Harigaya (unpublished).
[17] Y. Wang and L. T. Cheng, J. Phys. Chem. **96**, 1530 (1992).
[18] K. M. Creegan, J. L. Robbins, W. K. Robbins, J. M. Millar, R. D. Sherwood, P. J. Tindall, and D. M. Cox, J. Am. Chem. Soc. **114**, 1103 (1992).
[19] J. Shumway and S. Satpathy, Chem. Phys. Lett. **211**, 595 (1993).
[20] S. Leach *et al.*, Chem. Phys. **160**, 451 (1992).
[21] M. I. Salkola, Phys. Rev. B **49**, 4407 (1994).
[22] M. Yoshida and E. Osawa (unpublished); M. Yoshida and E. Osawa, The Japan Chemistry Program Exchange, Program No. 74.
[23] M. Fujita, R. Saito, G. Dresselhaus, and M. S. Dresselhaus, Phys. Rev. B **45**, 13 834 (1992).

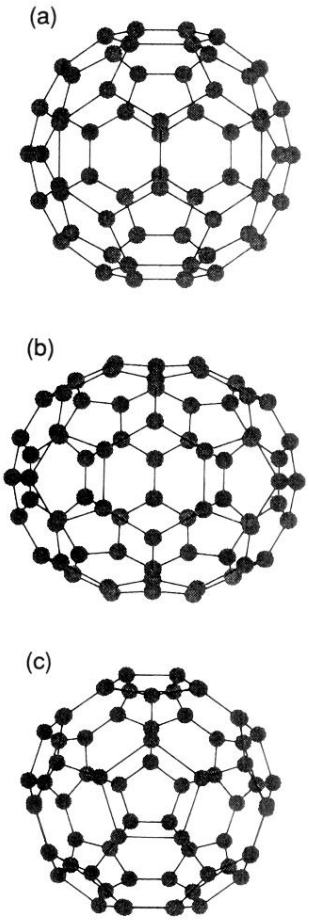

FIG. 1. Molecular structures for (a) C_{60}, and (b) and (c) C_{70}. In (b), the long axis (x axis) penetrates from the left to the right of the figure. The mirror symmetry planes are perpendicular to the figure. In (c), the C_{70} is projected along the long axis.